Energy Proceedings
Vol 59, 2025
ISSN 2004-2965

Techno-Economic Analysis of Seasonal Thermal Energy Storage in Local Multi-Energy Systems#

Boyuan Liu[1], Jiahao Ma[1], Zeyang Long[1], Xueyuan Cui[1], Yi Wang[1*]

Department of Electrical and Electronic Engineering, the University of Hong Kong, Hong Kong SAR, China

(Corresponding Author: yiwang@eee.hku.hk)

ABSTRACT

Local multi-energy systems can accommodate renewable energy while meeting the multi-energy demands of urban end-users. However, a seasonal imbalance exists between renewable energy supply and multi-energy demand. Seasonal thermal energy storage (STES) can efficiently address the seasonal imbalance, but whether or how much to install costly STES remains a question. To this end, this paper conducts a techno-economic analysis of STES. Three Chinese cities in different climate regions are selected for our analysis to find out in what situations STES is cost-effective and to understand why STES performs differently across cities. The result shows that STES is more economical in high-latitude cities with an intense seasonal heating difference. Exceedingly, alteration in STES capacity is attributed to the influence of the heat and cooling load ratio and carbon price.

Keywords: seasonal thermal energy storage, techno-economic analysis, multi-energy systems

1. INTRODUCTION

In the global low-carbon transition, local multi-energy systems (MESs) have emerged as an efficient approach to match distributed renewable energy and the multi-energy demands of urban end-users[1] . However, there is a seasonal mismatch between distributed solar generation and heat demand, forcing local energy systems to revert to fossil fuels during peak heat demand in winter. To address this challenge, Seasonal Thermal Energy Storage (STES) offers an effective solution by storing surplus solar energy generated during the summer underground and releasing it to meet peak heat demand in the winter[2] Given the temperature differential between STES and the local heating system, a ground source heat pump is typically integrated to enable efficient charging and discharging of STES [3]

Recent research has focused on two key areas to promote the adoption of STES: 1) improving STES techno-economic performance, and 2) integrating STES with local MESs. To improve the techno-economic performance of STES, Tafuni et al.[4] investigated various volume and shape designs of a cylindrical STES pit for local heating demands. Yang et al.[5] analyzed the techno-economic parameters of different types of STES and developed a decision tree to choose an appropriate type of STES in various scenarios. Regarding integrating with MESs, Zhou et al.[6] coupled STES with heat pumps and solar collectors and planned an MES in northern China; Mckenna et al.[7] evaluated the potential of STES to enhance the use of renewable energy in residential heating via planning across several German cities; Wei et al.[8] proposed a model predictive control strategy for the STES system in a district heating network.

While STES effectively addresses seasonal energy mismatches, its high investment costs and long payback periods make adoption challenging in local MESs. To determine the suitable scenarios for the STES application, a techno-economic analysis is necessary. Given the distinct renewable generation and heating demand profiles in various climate zones, the analysis should evaluate the economic benefits of STES in MESs across various cities [9] However, existing studies lack such cross-city comparisons, leaving unclear the scenarios when installing STES would be profitable and the reasons behind that.

To address the aforementioned research gap, this paper performs a techno-economic analysis of STES in local MESs in different cities to determine when and why STES would be cost-effective. The contribution of this paper is twofold:

(1) To find out in what situation STES is cost-effective, we examined the optimal capacities and scheduling strategies for commercial users in three typical Chinese cities with different climate zones. The

This is a paper for the 11th Applied Energy Symposium: Low Carbon Cities & Urban Energy Systems (CUE2025), July 18-22, 2024, Kitakyushu, Japan.

results show that STES is more economical in high-latitude cities with significant seasonal heat demand variations, but not in low-latitude cities where cooling demand dominates. Both seasonal and weekly patterns are found in the optimal energy transfer of STES.

(2) To understand why STES performs differently across cities, we analyzed its optimal capacities based on two key factors: 1) the heat and cooling load ratio in the total energy demand, and 2) the carbon price. The results show that in low-latitude cities, the capacity of STES increases as the heat and cooling load ratio rises, while in high-latitude cities, the optimal STES capacities remain unaffected by this ratio. After China's carbon price rises to European levels, the advantage of STES in high-latitude cities diminishes compared to low-latitude cities.

2. ANALYSIS METHOD OF OPTIMAL CONFIGURATION IN A LOCAL MES WITH STES

As shown in Fig. 1, the optimal configuration of a local MES with STES is analyzed based on the energy bus model [10] . The optimization model involving energy converters, energy storage devices, and STES is detailed as follows.

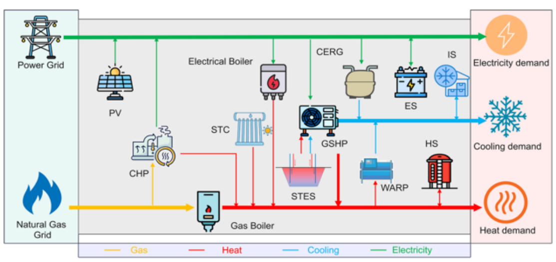

Fig. 1 Illustration of the energy bus model for the local MES with STES

2.1 Energy converters

For energy converters, the output power is proportional to the input power as:

$$\eta_{g,j} P_{g,j_{\text{in}},t}^{\text{in}} = P_{g,j,t}^{\text{out}}, \forall t, \forall g \in \Omega_c \quad (1)$$

where $\eta_{g,j}$ denotes the efficiency for the jth kind of output energy of the gth energy converter in the converter set Ω_c; $P_{g,j_{\text{in}},t}^{\text{in}}$ and $P_{g,j,t}^{\text{out}}$ respectively denotes the input and output power for the energy converter during the hour t. The candidate converter includes Combined Heat and Power (CHP), Electrical Boiler, Gas Boiler, Compression Electric Refrigerator Group (CERG), Ground Source Heat Pump (GSHP), and Water Absorption Refrigerator Group (WARP).

The capacity of the converter device $P_g^{\max}$ is defined as the maximum input power and is defined as:

$$P_{g,j_{\text{in}},t}^{\text{in}} \leq P_g^{\max}, \forall t, \forall g \in \Omega_c \quad (2)$$

2.2 Energy storage devices

The state of charge (SOC) transition for short-term storage is formulated as:

$$\text{SOC}_{g,t} = (1-\alpha_g)\text{SOC}_{g,t-1} + P_{g,t}^{+}\eta_g^{+} - \frac{P_{g,t}^{-}}{\eta_g^{-}}, \forall g \in \Omega_{\text{ss}} \quad (3)$$

where η_g^+ and η_g^- respectively denote the charging and discharge efficiency for the gth energy storage in the short-term storage set Ω_{ss}; α_g denotes the hourly self-discharge rate; $P_{g,t}^-$ and $P_{g,t}^+$ are the charging and discharging power.

The capacity of short-term storage $E_g^{\max}$ is defined as the maximum stored energy:

$$\text{SOC}_{g,t} \leq E_g^{\max}, \forall t, \forall g \in \Omega_{\text{ss}} \quad (4)$$

We assume that short-term storage follows the daily cycle during operation:

$$\text{SOC}_{g,t=24n} = \text{SOC}_{g,t=24(n+1)}, \forall g \in \Omega_{ss} \quad (5)$$

Where n is the index for the operating day.

The relationship between the maximum power and the stored energy is established by introducing the duration time T_g, formulated as:

$$P_{g,t}^{+} \leq \frac{E_g^{\max}}{T_g}, \forall t, \forall g \in \Omega_{\text{ss}} \quad (6a)$$

$$P_{g,t}^{-} \leq \frac{E_g^{\max}}{T_g}, \forall t, g \in \Omega_{\text{ss}} \quad (6b)$$

2.3 The STES system

The candidate STES system is a Tank Thermal Energy Storage (TTES) coupled with GSHP. Besides the conversion efficiency and capacity constraints stated in Eqs. (1) and (2), GSHP is not allowed to operate in heating and cooling states at the same time:

$$P_{\text{GSHP,cool},t}^{\text{out}} \leq x_{\text{GSHP},t}^{\text{cool}} M, \forall t \quad (7a)$$

$$P_{\text{GSHP,heat},t}^{\text{out}} \leq x_{\text{GSHP},t}^{\text{heat}} M, \forall t \quad (7b)$$

$$x_{\text{GSHP},t}^{\text{cool}} + x_{\text{GSHP},t}^{\text{heat}} \leq 1 \quad (7c)$$

where $P_{\text{GSHP,cool},t}^{\text{out}}$ and $P_{\text{GSHP,heat},t}^{\text{out}}$ stand for the cooling and heating power of GSHP; $x_{\text{GSHP},t}^{\text{cool}}$ and $x_{\text{GSHP},t}^{\text{heat}}$ are binary variables for the cooling and heating state of GSHP; M is a large coefficient.

The energy flow inside the STES system is as follows:

$$\begin{aligned} P_{\text{GSHP,elec},t}^{\text{in}} + P_{\text{GSHP,cool},t}^{\text{out}} - P_{\text{GSHP,heat},t}^{\text{out}} \\ = P_{\text{STES},t}^{+} - P_{\text{STES},t}^{-} \end{aligned} \quad (8)$$

where $P_{\text{GSHP,elec},t}^{\text{in}}$ is the consumed electrical power of GSHP; $P_{\text{STES},t}^{+}$ and $P_{\text{STES},t}^{-}$ are the charging and discharging power of STES. Combined with Eq. (1), the relationship between the charging and discharging power of STES and the consumed electrical power of GSHP is formulated as:

$$P_{\mathrm{STES},t}^{+} = (\eta_{\mathrm{STES,cool}} + 1) P_{\mathrm{GSHP,elec}}^{\mathrm{in}} \quad (9a)$$

$$P_{\mathrm{STES},t}^{-} = (\eta_{\mathrm{STES,heat}} - 1) P_{\mathrm{GSHP,elec}}^{\mathrm{in}} \quad (9b)$$

The SOC transition of STES is formulated by:

$$\mathrm{SOC}_{\mathrm{STES},t} = (1-\alpha_{\mathrm{STES}})\mathrm{SOC}_{\mathrm{STES},t-1} + P_{\mathrm{STES},t}^{+}\eta_{\mathrm{STES}}^{+} - \frac{P_{\mathrm{STES},t}^{-}}{\eta_{\mathrm{STES}}^{-}} + P_{\mathrm{STES,heat},t}^{\mathrm{in}} \quad (10)$$

where $P_{\mathrm{STES,heat},t}^{\mathrm{in}}$ denotes the surplus heat absorbed by STES from the heating system.

To guarantee a sustainable operation, STES should follow a yearly SOC cycle:

$$\mathrm{SOC}_{\mathrm{STES},t=0} = \mathrm{SOC}_{\mathrm{STES},t=8760} \quad (11)$$

2.4 Solar devices

Candidate solar devices include solar thermal collectors (STC) and photovoltaic (PV) panels. The generation power of solar devices is modeled as:

$$P_{g,j,t}^{\mathrm{solar}} \le A_g I_t \beta_g, \forall t, \forall g \in \Omega_{sl} \quad (12)$$

where A_g denotes the construction area of the gth solar device in the solar device set Ω_{sl}; I_t represents the normalized solar irradiation intensity profile; β_g represents the maximum generation capacity per square kilometer.

2.5 Energy bus balance

The input and output power on each energy bus for the whole system concerning time t are balanced. For each kind of energy carrier j, we have:

$$P_{j,t}^{\mathrm{buy}} + \sum_{g\in\Omega_c,\{\mathrm{STES}\}} (P_{g,j,t}^{\mathrm{out}} - P_{g,j,t}^{\mathrm{in}}) + \sum_{g\in\Omega_{ss}} (P_{g,t}^{-} - P_{g,t}^{+}) + P_{g,j,t}^{\mathrm{solar}} = P_{j,t}^{\mathrm{load}} \quad (13)$$

where the output load demand $P_{j,t}^{\mathrm{load}}$ is balanced with energy obtained from the grid $P_{j,t}^{\mathrm{buy}}$, energy output or input from candidate conversion and storage devices, and solar energy generation.

2.6 Objective function

The objective function is to minimize the annual investment cost C^{inv} and the operation cost C^{opr}:

$$\min C^{\mathrm{inv}} + C^{\mathrm{opr}} \quad (14)$$

where the annual investment cost C^{inv} is calculated as follows:

$$C^{\mathrm{inv}} = C^{c} + C^{\mathrm{ss}} + C^{sl} + C_0^{\mathrm{STES}} \quad (15a)$$

$$C^{c} = \sum_{g\in\Omega_c} \frac{i}{1-(1+i)^{-Y_g}} c_g^{c} P_g^{\max} \quad (15b)$$

$$C^{ss} = \sum_{g\in\Omega_s,\{\mathrm{STES}\}} \frac{i}{1-(1+i)^{-Y_g}} c_g^{\mathrm{ss}} E_g^{\max} \quad (15c)$$

$$C^{sl} = \sum_{g\in\Omega_{sl}} \frac{i}{1-(1+i)^{-Y_g}} c_g^{\mathrm{sl}} A_g \beta_g \quad (15d)$$

where i stands for the expected discount rate; Y_g denotes the life span of the gth device; $c_g^{c}, c_g^{\mathrm{ss}}, c_g^{\mathrm{sl}}$ are the unit capacity costs for converters, storage devices, and solar devices.

In addition, STES has a relatively high fixed installation cost if built, which is formulated as:

$$C_0^{\mathrm{STES}} = z^{\mathrm{STES}} c_0^{\mathrm{STES}} \quad (16a)$$

$$E_{\mathrm{STES}}^{\max} \le M z^{\mathrm{STES}}, \forall t, z^{\mathrm{STES}} \in \{0,1\} \quad (16b)$$

where z^{STES} is a binary variable denoting whether STES is used in the local MES.

The operation cost C^{opr} is formulated as:

$$C^{\mathrm{opr}} = C^{\mathrm{buy}} + C^{\mathrm{CO_2}} \quad (17a)$$

$$C^{\mathrm{buy}} = \sum_t c_{\mathrm{elec}}^{\mathrm{buy}} P_{\mathrm{elec},t} + c_{\mathrm{gas}}^{\mathrm{buy}} P_{\mathrm{gas},t} \quad (17b)$$

$$C^{\mathrm{CO_2}} = c^{\mathrm{CO_2}} \sum_t e_{\mathrm{elec}}^{\mathrm{CO_2}} P_{\mathrm{elec},t} + e_{\mathrm{gas}}^{\mathrm{CO_2}} P_{\mathrm{gas},t} \quad (17c)$$

where C^{buy} and $C^{\mathrm{CO_2}}$ are the total costs for importing energy from and the carbon emission; $c_{\mathrm{elec}}^{\mathrm{buy}}$ and $c_{\mathrm{gas}}^{\mathrm{buy}}$ are respectively the unit cost of importing electricity and gas; $e_{\mathrm{elec}}^{\mathrm{CO_2}}$ and $e_{\mathrm{gas}}^{\mathrm{CO_2}}$ denote the carbon emission factors of using electricity and gas; $c^{\mathrm{CO_2}}$ is the carbon emission price.

3. EMPIRICAL ANALYSIS OF CITIES ACROSS DIFFERENT LATITUDES IN CHINA

3.1 Experimental setups

We utilize various types of data, including building footprints [11] and meteorological data [12] , and employ a simulation tool [13] to generate the power generation curve of rooftop PV in cities. Besides, DeST [14] serves as the simulation engine to generate heat, cooling, and electrical energy demands in building prototypes, which are scaled up to get the city-level results based on the building footprint area, as illustrated in Fig. 2. The electricity load for the three cities is normalized to 100MW, while the cooling and heat demands differ. Referenced from [7] [15], the operating characteristics of the devices used in the experiment are listed in Table 1 and Table 2, respectively.

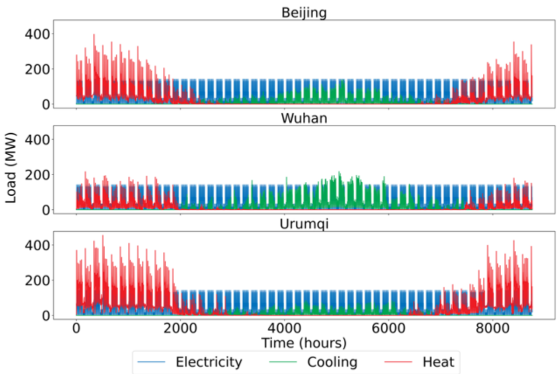

Fig. 2 Electricity, heat, and cooling load of the three cities' MES in the planning year

Table 1 Energy characteristics for the candidate energy storage device

Device	Self-Discharge Rate (h^{-1})	Duration (h)
Elec Storage	0.00054	2
Heat Storage	0.0075	5
Ice Storage	0.0075	5
STES	**0.00001**	**1**

Table 2 Parameters of the candidate devices

Device	Efficiency	Investment Cost (million RMB/MW), Life Span (Year)
PV	0.83	1020, 25
STC	0.75	604, 20
GSHP (η_h, η_c)	**3.4, 4.6**	**330, 20**
STES	**0.75**	**1.1325, 30, 116.324(installation)**
CHP (η_e, η_h)	0.22, 0.7	773.03, 30
Gas Boiler	0.85	44, 20
Electric Boiler	0.85	55.48, 20
CERG	3.5	123.37,15
WARP	1.2	86.14, 20
Elec Storage	0.9487	228,10
Heat Storage	0.894	11, 25
Ice Storage	0.894	11, 25

3.2 Comparison of planned configuration results

As shown in Table 3, the optimal results vary between cities. Low-latitude cities like Wuhan utilize more CERG and WARP to satisfy the cooling demand. In contrast, Beijing and Urumqi are heat-directed with significantly more GSHP. Exceedingly, as illustrated in Fig. 2, a greater seasonal imbalance of heat demand results in more planning of STES, which is attributed to the STES heat storing principle: Higher heat demand cities like Beijing and Urumqi utilize more STES than Wuhan to collect heat during the cooling season and therefore address the heat demand seasonally.

Table 3 Optimal planning results for cities with a carbon price of 100RMB/tCO_2

Device (MW)	Beijing	Wuhan	Urumqi
PV (km^2)	0.168	0.146	0.126
STC (km^2)	0.0	0.0	0.0
GSHP	**8.9**	**3.7**	**9.4**
STES	**1020.9**	**425.0**	**1086.6**
CHP	172.2	207.0	207.8
Gas Boiler	52.5	0.0	59.2
Electric Boiler	6.4	0.0	13.4
CERG	0.0	5.3	0.0
WARP	45.5	75.5	28.6
Elec Storage	26.2	36.1	29.4
Heat Storage	204.5	223.3	226.0
Ice Storage	63.6	140.2	57.5

3.3 Comparison of STES's optimal scheduling results

Heat and cooling loads can be considered collectively as WARP allows transformation. Correspondingly, the SOC plot of the optimal STES scheduling result shown in Fig. 3 resembles the integrated heat-cooling load graph in Fig. 2: Beijing is identical to Urumqi, and both display two peaks, while Wuhan shows small operation cycles year-round.

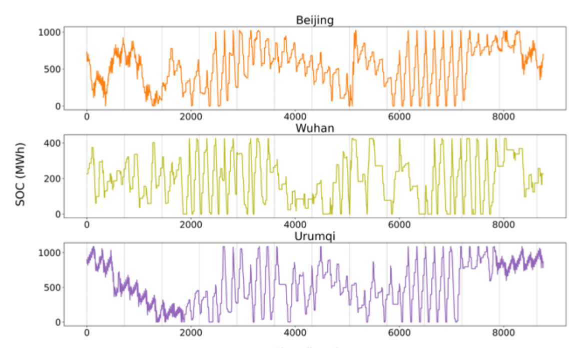

Fig. 3 The state of charge of the STES in a year for the three cities

Additionally, there are four peaks each month, on account of the demand difference between weekdays and weekends. On weekdays when all demands are high, the optimal solution tends to utilize CHP to balance the heat and electricity demand simultaneously, while on weekends with less electricity demand and settled heat demand, there occurs less CHP utility and supplementary for heating by STES discharge.

4. LOCAL SENSITIVITY ANALYSIS ON STES CAPACITY

4.1 Impact of multi-energy demand

When scaling heat and cooling loads between 5% and +5%, cities show varied responses in Fig. 4. Wuhan exhibits an overall increase in STES capacity. Beijing's STES capacity remains stable with minor fluctuations. In Urumqi, STES capacity peaks at -1%, driven by higher heat and cooling demand. When further scaled, as the heat demand exceeds cooling demand significantly, the tendency for heating results in more boiler capacity, increasing from 57.38 MW (at the -1% case) to 70.11 MW (at the 5% case), which necessitates fewer STES and creates a downward trend in STES capacity.

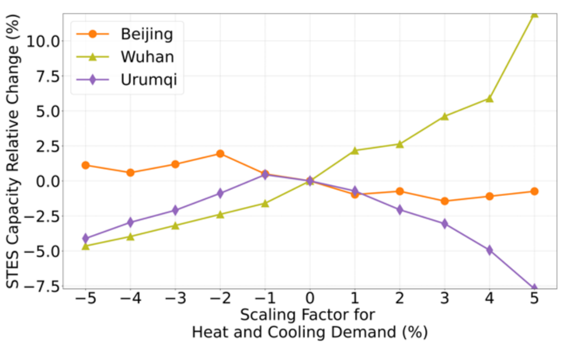

Fig. 4 The alteration of STES capacity relative change in the three cities 'planning result when the scale of the load varies between (-5%-5%)

4.2 Impact of the carbon price

The standard carbon price varies between regions; China commonly falls around 100 (RMB/tCO_2) while the European Union remains around 600 (RMB/tCO_2).

A sensitivity analysis for a carbon price is carried out and a counterintuitive alteration of STES to expectation took place when the price of carbon per unit output altered (shown in Fig. 5): the STES capacity of the three cities shares a descending trend when the carbon price increases.

Using Beijing with carbon prices of 100 & 600 (RMB/tCO_2) as a case study, shown in Fig. 6. Net loads are calculated by transforming the cool demand satisfied by WARP to heat demand and subtracting the heat produced by the solar thermal collector. The net load for price-100 cases is positive, while the net heat load is negative in the price-600 case and is generally larger than the net cold demand. This implies that when the carbon price is high, investment in solar devices is more economical than building STES, potentially resulting in a descending trend in STES capacity.

The paper proposes a techno-economic analysis to

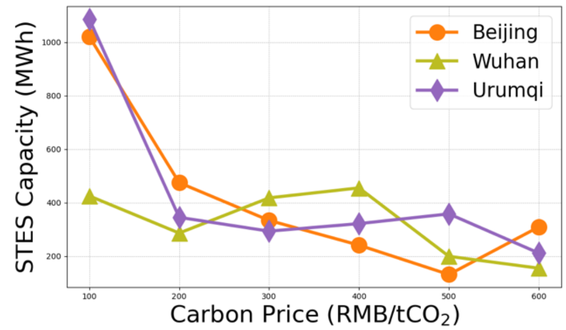

Fig. 5 The alteration of STES capacity in the three cities 'planning result when the carbon price (RMB/tCO_2) increases from 100 to 600

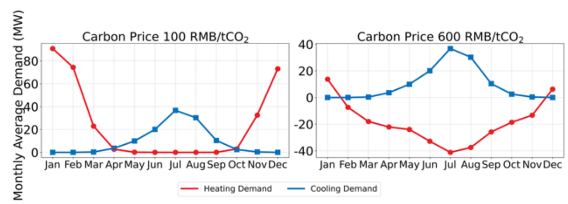

Fig. 6 The net heat demand and net cool demand per month of Beijing in the planning year when the carbon price is 100 & 600 (RMB/tCO_2)

implement the vacancy of cross-regional and multi-scenario comparison of STES economic benefits. To find when STES is cost-effective, a comparison of the three cities is carried out. The result that high-latitude cities like Beijing and Guangzhou store more STES implies that higher seasonal heat demand difference stimulates STES capacity growth. In addition, the SOC of STES follows the seasonal and weekly distribution of heat and cooling integrated load (on account of WARP's transformation), peaking at high demand time and maintaining four small peaks monthly due to weekday & weekend load differences.

The varying factor that influences STES performance is attributed to the carbon price as well as the heat and cooling demand ratio in total demand. When carbon prices ascend, STES capacity decreases due to the alternative investment in more efficient solar devices; when the heat and cooling demand ratio in total demand ascends, STES capacity increases in low-latitude cities like Wuhan, while remaining basically stable in high-latitude cities like Beijing.

Further work on the techno-economic analysis of STES should involve two key aspects. First, a broader range of scenarios and various technical boundary conditions will be considered to obtain a more comprehensive understanding of STES's techno-economic characteristics. Second, an analysis will be conducted on the integration of STES with the MES system, aiming to quantify the factors influencing STES efficiency.

ACKNOWLEDGEMENT

This work was supported in part by the National Key Research and Development Program of China under Grant 2022YFE0141200 and in part by the Research Grants Council of the Hong Kong SAR under Grant HKU 27203723.

REFERENCE

[1] Bahlawan, H., Losi, E., Manservigi, L., Morini, M., Pinelli, M., Spina, P. R., & Venturini, M. (2022). Optimization of a renewable energy plant with seasonal energy storage for the transition towards 100% renewable energy supply. Renewable Energy, 198, 1296-1306.

[2] Lyden, A., Brown, C. S., Kolo, I., Falcone, G., & Friedrich, D. (2022). Seasonal thermal energy storage in smart energy systems: District-level applications and modelling approaches. Renewable and Sustainable Energy Reviews, 167, 112760.

[3] Gao, D., Kwan, T. H., Hu, M., & Pei, G. (2022). The energy, exergy, and techno-economic analysis of a solar seasonal residual energy utilization system. Energy, 248, 123626.

[4] Tafuni, A., Giannotta, A., Mersch, M., Pantaleo, A. M., Amirante, R., Markides, C. N., & De Palma, P. (2023). Thermo-economic analysis of a low-cost greenhouse thermal solar plant with seasonal energy storage. Energy Conversion and Management, 288, 117123.

[5] Yang, T., Liu, W., Kramer, G. J., & Sun, Q. (2021). Seasonal thermal energy storage: A techno-economic literature review. Renewable and Sustainable Energy Reviews, 139, 110732.

[6] Zhou, Y., Min, C., Wang, K., Xie, L., & Fan, Y. (2023). Optimization of integrated energy systems considering seasonal thermal energy storage. Journal of Energy Storage, 71, 108094.

[7] McKenna, R., Fehrenbach, D., & Merkel, E. (2019). The role of seasonal thermal energy storage in increasing renewable heating shares: A techno-economic analysis for a typical residential district. Energy and Buildings, 187, 38-49.

[8] Wei, Z., Tien, P. W., Calautit, J., Darkwa, J., Worall, M., & Boukhanouf, R. (2024). Investigation of a model predictive control (MPC) strategy for seasonal thermochemical energy storage systems in district heating networks. Applied Energy, 376, 124164.

[9] Yang, T., Liu, W., Sun, Q., Hu, W., & Kramer, G. J. (2023). Techno-economic-environmental analysis of seasonal thermal energy storage with solar heating for residential heating in China. Energy, 283, 128389.

[10] Xia, T., Huang, W., Lu, X., Zhang, N., & Kang, C. (2020). Planning district multiple energy systems considering year-round operation. Energy, 213, 118829.

[11] Sun X, Huang X, Mao Y, et al. GABLE: A first fine-grained 3D building model of China on a national scale from very high resolution satellite imagery[J]. Remote Sensing of Environment, 2024, 305: 114057.

[12] European Centre for Medium-Range Weather Forecasts. (n.d.). ECMWF data services. https://ecds-prod.ecmwf.int/

[13] Lindberg F, Jonsson P, Honjo T, Wästberg D 2015: Solar energy on building envelopes - 3D modelling in a 2D environment. Solar Energy. 115, 369 – 378

[14] Yan D, Zhou X, An J, et al. DeST 3.0: A new-generation building performance simulation platform. Build Simul. 2022;15 (11):1849-1868. doi:10.1007/s12273-022-0909-9

[15] Petkov, I., & Gabrielli, P. (2020). Power-to-hydrogen as seasonal energy storage: an uncertainty analysis for optimal design of low-carbon multi-energy systems. Applied Energy, 274, 115197.